Infrared Physics & Technology 89 (2018) 299–303

Contents lists available at ScienceDirect

Infrared Physics & Technology

journal homepage: www.elsevier.com/locate/infrared

Regular article

Thermal effects of an ICL-based mid-infrared CH_4 sensor within a wide atmospheric temperature range

Weilin Ye [a,b], Chuantao Zheng [c,*], Nancy P. Sanchez [d], Aswathy V. Girija [b], Qixin He [b,c], Huadan Zheng [b], Robert J. Griffin [d], Frank K. Tittel [b]

[a] Intelligent Manufacturing Key Laboratory of Ministry of Education, College of Engineering, Shantou University, 243 Daxue Road, Shantou 515063, PR China
[b] Electrical and Computer Engineering Department, Rice University, 6100 Main Street, Houston, TX 77005, USA
[c] State Key Laboratory of Integrated Optoelectronics, College of Electronic Science and Engineering, Jilin University, 2699 Qianjin Street, Changchun 130012, PR China
[d] Department of Civil and Environmental Engineering, Rice University, 6100 Main Street, Houston, TX 77005, USA

HIGHLIGHTS

- Study of thermal effects of an ICL-based mid-infrared methane sensor.
- A LabVIEW-based program was developed to study thermal effects based on infrared absorption spectroscopy.
- A temperature compensation technique was developed to control thermal effects.
- CH_4 measurements were conducted within a wide range of atmospheric temperature.

ARTICLE INFO

Article history:
Received 23 October 2017
Revised 13 January 2018
Accepted 15 January 2018

Keywords:
Laser sensors
Infrared spectroscopy
Thermal effects
Temperature compensation

ABSTRACT

The thermal effects of an interband cascade laser (ICL) based mid-infrared methane (CH_4) sensor that uses long-path absorption spectroscopy were studied. The sensor performance in the laboratory at a constant temperature of ~25 °C was measured for 5 h and its Allan deviation was ~2 ppbv with a 1 s averaging time. A LabVIEW-based simulation program was developed to study thermal effects on infrared absorption and a temperature compensation technique was developed to minimize these effects. An environmental test chamber was employed to investigate the thermal effects that occur in the sensor system with variation of the test chamber temperature between 10 and 30 °C. The thermal response of the sensor in a laboratory setting was observed using a 2.1 ppm CH_4 standard gas sample. Indoor/outdoor CH_4 measurements were conducted to evaluate the sensor performance within a wide atmospheric temperature range.

1. Introduction

Methane (CH_4) is a potent greenhouse gas that causes instantaneous radiative forcing [1]. The Intergovernmental Panel on Climate Change indicates that anthropogenic CH_4 emissions have increased over the last three decades and the atmospheric mixing ratio of CH_4 increased from 722 ± 25 ppb in 1750 to 1802 ± 25 ppb in 2011 [2]. A wide range of anthropogenic activities lead to the increasing emission of CH_4. The US Environmental Protection Agency reports that the largest sources of anthropogenic CH_4 emissions are natural gas and petroleum systems followed by fermentation processes [3,4]. Considering the relevance of CH_4 from an environmental and safety perspective, the development of sensitive and reliable sensor systems for monitoring real-time CH_4 concentrations in the atmosphere is necessary.

Infrared laser absorption spectroscopy (IR-LAS) sensors play an important role in high-resolution atmospheric trace gas diagnostics. There are various IR-LAS techniques such as direct absorption spectroscopy (DAS), wavelength modulation spectroscopy (WMS) and frequency modulation spectroscopy (FMS) [5–7]. Infrared absorption depends on the gas pressure and temperature. In order to obtain good stability in measurements, strict control of these two parameters is required. Unlike the pressure control achieved with commercial pressure controllers, temperature control is often difficult or not feasible for large multi-pass gas cell (MPGC) based gas sensors due to temperature effects on the mechanical system, electronics and optics, especially when the sensor is used in an environment with a wide temperature range. Although a CH_4

* Corresponding author.
E-mail address: zhengchuantao@jlu.edu.cn (C. Zheng).

https://doi.org/10.1016/j.infrared.2018.01.017
1350-4495/

sensor possesses satisfactory performance in laboratory settings [8–10], it may not be suitable for operation in harsh environments.

In this work, we report the thermal behavior of the sensor performance of a previously reported CH_4 sensor based on long-path, mid-infrared absorption spectroscopy [11,12]. A LabVIEW program was developed to simulate variations of the CH_4 absorption with temperature. An environmental test chamber was utilized to investigate the sensor performance for a wide range of temperatures. Both absorption and non-absorption factors responsible for the thermal behavior of the sensor were investigated theoretically through laboratory tests and outdoor CH_4 measurements.

2. Sensor structure and laboratory performance

2.1. Absorption line selection

According to the high-resolution transmission (HITRAN) database [13], the absorption spectra of 2% H_2O and 2 ppm CH_4 at a pressure of 760 Torr, an effective optical path length of 5460 cm and a temperature of 300 K are depicted in Fig. 1(a). Two H_2O absorption peaks at 3334.28 nm and 3334.47 nm are observed, which overlap with the CH_4 absorption peak at 3334.45 nm. In order to minimize the broadening of these absorption lines, the pressure in the MPGC is reduced to 100 Torr, as shown in Fig. 1 (b). One of the CH_4 absorption lines at 3334.38 nm without any effect from H_2O is separated into two lines at 100 Torr and the other CH_4 line occurs at 3334.46 nm. Therefore, the interference-free CH_4 absorption line centered at 3334.38 nm was selected as the optimum target line.

2.2. Sensor architecture with temperature monitor

A mid-infrared laser based sensor system using long-path absorption spectroscopy was developed for the detection of CH_4 (Fig. 2). A continuous wave (CW), distributed feedback (DFB) ICL centered at 3337 nm (Nanoplus, Germany) was used as the mid-infrared laser source. The laser beam was coupled into a compact MPGC with an optical path length of 54.6 m by a mode matching lens (L) and two plane mirrors (M1 and M2). The beam was focused into a mercury-cadmium-telluride (MCT) infrared detector (PVI-4TTE-3.4, Vigo Systems, Poland) with optimal detection at 3400 nm using a parabolic mirror (PM). A compact, custom laser current driver (CD, with dimensions of $4.2 \times 4.8\ cm^2$) and temperature

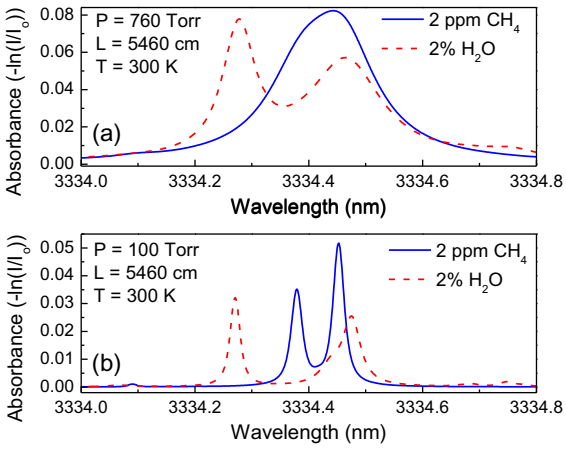

Fig. 1. HITRAN-based absorption spectra of H_2O (2%) and CH_4 (2 ppm) in a narrow spectral range. The absorption lines of H_2O and CH_4 are shown in red and blue respectively. Wavenumber range is from 3334.0 nm to 3334.8 nm for a 5460 cm path length at a pressure of (a) 760 Torr and (b) 100 Torr.

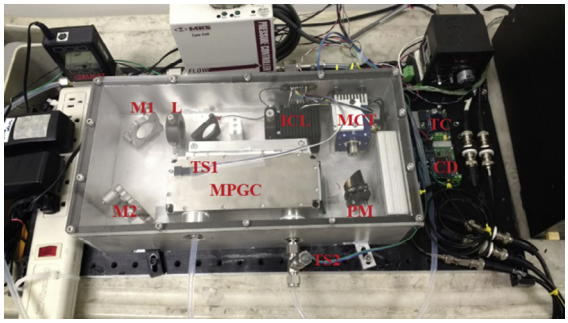

Fig. 2. Photograph of the CH_4 sensor system, which includes an optical sensor core enclosed in a box, a gas flow meter, a pressure controller and electronics for laser driver and temperature controller. The laptop and data acquisition card are not shown here.

controller (TC, with dimensions of $4.5 \times 3.6\ cm^2$) were used for the ICL operation. In order to keep the pressure at a constant value inside the MPGC, a pressure controller (649A, MKS Instruments Inc, MA) and a vacuum pump (N 813.5 ANE/AF, KNF Neuberger Inc, NJ) were employed. Two precision centigrade temperature sensors (TS1 and TS2, LM35, Texas Instruments, USA) were placed inside and outside the MPGC to record the real-time temperature of the target gas (related to absorbance) and the temperature in the optical core of the sensor system, respectively.

2.3. Sensor performance in laboratory tests

CH_4 concentration measurements using a 2.1 ppm standard sample (Airgas Company, Houston, TX, USA) and temperatures of the target gas were acquired for a period of ~5 h in a laboratory setting (constant temperature ~25 °C). The blue and red traces presented in Fig. 3(a) show a total variation range of the measured concentration of ±30 ppb for ~5 h observation time. Both concentration and temperature measurements have a low-frequency fluctuation probably caused by AC power-frequency interference induced by other equipment in the laboratory. An Allen-Werle analysis was utilized to evaluate the stability of the CH_4 sensor based on the measured data. As shown in Fig. 3(b), the Allan deviation was plotted on a log-log scale versus the averaging time. Unlike a typical Allan deviation plot, the Allan deviation starts to increase at an averaging time of several seconds, due to the absorption spectral averaging in the LabVIEW program before absorption line fitting. This means that the processing in the program has successfully suppressed the White-Gaussian noise and the further data averaging causes no effect. The plot indicates a measurement precision of ~2 ppb with a 1 s averaging time.

3. Thermal effects and compensation

3.1. Theoretical analysis

The transmission of infrared light at frequency υ through a uniform absorbing medium of length L follows the Beer-Lambert law, as

$$\tau(\nu) = I(\nu)/I_0 = \exp[-\alpha(\nu)CL], \quad (1)$$

where C is the volume ratio of the absorption gas, $\tau(\upsilon)$ is the transmissivity at frequency υ, I_0 is the output intensity, $I(\upsilon)$ is the intensity after passing through the absorbing medium with a length L, and $\alpha(\upsilon)$ is the spectral absorption coefficient which can be described as

$$\alpha(\nu) = P_{abs}S(T, \nu_0)\phi_\nu, \quad (2)$$

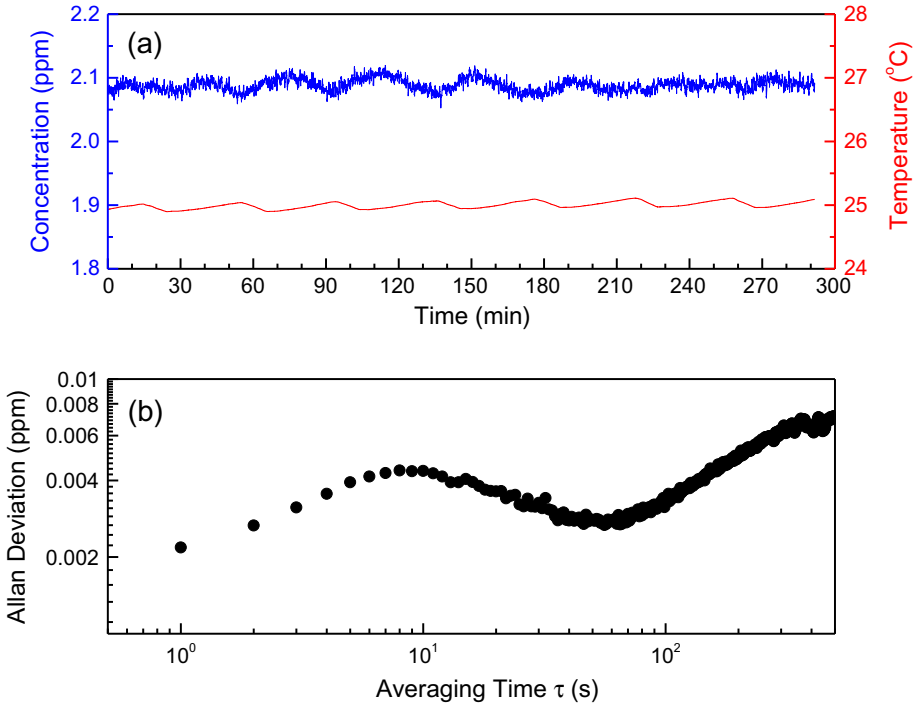

Fig. 3. (a) Concentration of CH_4 (blue) and the temperature inside the MPGC (red) of a 2.1 ppm sample measured during a laboratory test for ~5 h (Temperature ~25 °C). (b) An Allan deviation plot as a function of averaging time, based on the data shown in Fig. 3(a).

where P_{abs}(unit: atm) is the pressure of the absorbing medium, $S(T, \upsilon_0)$ (unit: $cm^{-2}\,atm^{-1}$) is the line-strength and ϕ_v(unit : cm) is the line shape function. The line-strength at any temperature T can be calculated from Eq. (3):

$$S(T,\nu_0) = S(T_0,\nu_0)\frac{T_0}{T}\frac{Q(T_0)}{Q(T)}\frac{1-\exp(-hc\nu_0/kT)}{1-\exp(-hc\nu_0/kT_0)} \times \exp\left[-\frac{hcE^*}{k}\left(\frac{1}{T}-\frac{1}{T_0}\right)\right] \quad (3)$$

where T(unit: K) is gas temperature, T_0(unit: K) is reference temperature, $Q(T)$ is the rovibrational partition function, h(unit: Js) is Planck's constant, c(unit: cm s^{-1}) is the speed of light, k(unit: J K^{-1}) is the Boltzmann's constant and E^*(unit: cm^{-1}) is the lower state energy [14].

3.2. Absorbance and second harmonic signal at different temperatures

As seen from Eq. (3), the line-strength $S(T,\upsilon_0)$ does not have a simple relation with temperature. Therefore, in order to investigate the sensor's thermal characteristics, a LabVIEW program was developed to simulate the CH_4 absorption spectra for different temperatures. All the parameters in the program are based on the CH_4 sensor setup described in Section 2.3. In order to obtain the 2f signal, a LabVIEW-based lock-in amplifier was employed. The 2f signal amplitude V_{2f} for 8 different CH_4 concentration levels (1, 2, 3, 4, 5, 6, 7 and 8 ppm) at 25 °C are shown in Fig. 4(a). A fitting curve between V_{2f} and a concentration level C was obtained as

$$C(\text{ppm}) = 368.57276 \times V_{2f}(C, 25^\circ\text{C}) - 0.02411 \quad (4)$$

For different temperatures ranging from 10 to 40 °C, for three CH_4 concentration levels (1, 2 and 3 ppm), the maximum voltage of 2f signal amplitude, considering concentration and temperature, was recorded and denoted as $V_{mea}(C,T)$. The relative error between $V_{mea}(C,T)$ and $V_{mea}(C,25^\circ\text{C})$ is given by Eq. (5)

$$E = (V_{mea}(C,T) - V_{2f}(C,25^\circ\text{C}))/V_{2f}(C,25^\circ\text{C}) \quad (5)$$

where $V(C,25^\circ\text{C})$ can be calculated from Eq. (4). The results of the relative error are shown in Fig. 4(b). From Fig. 4(b) the measured errors for different concentration levels almost overlap and can be fitted by Eq. (6)

$$E = 0.16 - 0.00628 \times T(^\circ\text{C}) \quad (6)$$

Therefore, with a measured 2f signal amplitude $V_{mea}(C,T)$ and a temperature T, we can obtain the compensated 2f signal amplitude as:

$$V_{2f}(C,25^\circ\text{C}) = \frac{V_{mea}(C,T)}{1+E} \quad (7)$$

Combining Eqs. (4), (6) and (7), we obtain a compensation equation for the concentration as

$$C(\text{ppm}) = 368.57276 \times V_{mea}(C,T)/(1.16 - 0.00628T) - 0.02411 \quad (8)$$

3.3. Absorbance compensation

Absorbance data of three CH_4 concentration levels (1, 2 and 3 ppm) from the HITRAN database at 7 different temperatures (10, 15, 20, 25, 30 35 and 40 °C) were used to study the thermal variation and compensation effect of the CH_4 sensor system. From the circle symbols in Fig. 4(c), we can see that when the temperature is changed from 10 to 40 °C, the relative variation of the measured results is ~18.2%, 18.9% and 19.7% for the concentration levels of 3, 2 and 1 ppm, respectively. Here, the relative variation (RV) is given by Eq. (9)

$$RV = (\text{Measured maximum} - \text{Measured minimum})/ \times \text{Target concentration} \quad (9)$$

According to Eq. (8), the compensation values of the concentration are shown as square symbols in Fig. 4(c). After compensation, the relative variation of the measured results reduced to 0.7%, 0.6%

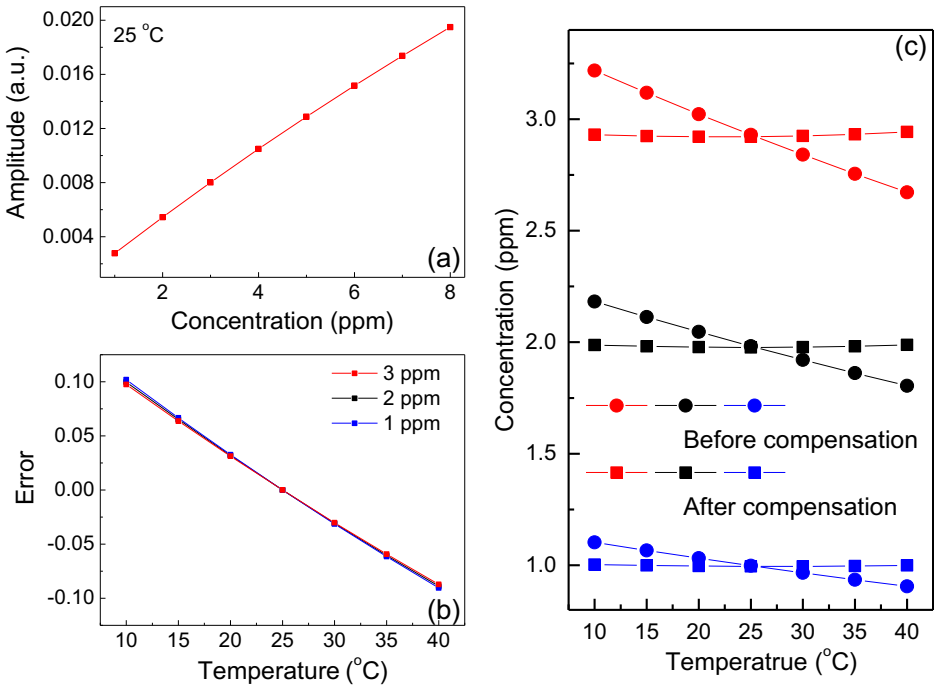

Fig. 4. (a) Measured 2*f* signal amplitude for 8 different CH_4 concentration levels (1, 2, 3, 4, 5, 6, 7 and 8 ppm) at 25 °C. (b) Measured relative error versus temperature. (c) Comparison of three CH_4 concentration levels (1, 2 and 3 ppm) before and after compensation.

and 0.7% at 3, 2 and 1 ppm respectively, which is considerably smaller than the values before compensation.

4. Indoor and outdoor thermal effect measurements

4.1. Indoor measurements

The CH_4 sensor was placed in an environmental test chamber (ESPEC, Walk-in series SCP-220) located in the Air Quality Research Group at Rice University. The chamber was operated in a constant temperature mode. A 2.1 ppm CH_4 standard cylinder was used to verify the variations of the CH_4 concentration levels. The temperature of the sensor system and the measured CH_4 concentrations are shown in Fig. 5(a) with variation of the test chamber temperature between 10 and 30 °C. Fig. 5(b) shows the relationship between measured concentration before and after the compensation. The measured concentration increased by ~70% (from 2 ppm to 3.5 ppm) as the temperature in the MPGC decreased by ~42% when the temperature drops from 24 °C to 14 °C.

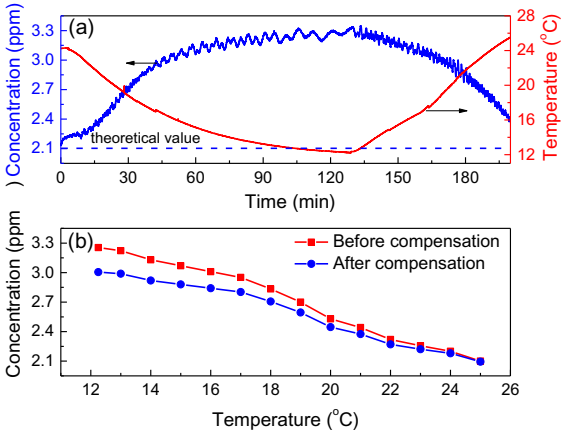

Fig. 5. (a) Temperature inside the MPGC and the CH_4 concentration measured during the experiment in the environmental chamber. (b) CH_4 concentration measured before and after temperature compensation using Eq. (8) as a function of temperature inside the MPGC, when only the thermal effects on infrared absorption are considered. In these measurements, a 2.1 ppm CH_4 standard cylinder was used to verify the variations of the CH_4 concentration levels.

Eq. (8) was used to compensate for the influence of temperature variations. There is an improvement with the compensation, due to the reduction in the fluctuation from 0.09358 ppm/°C to 0.08074 ppm/°C, which confirms that the compensation method is effective. The compensation result is shown in Fig. 5(b). The compensation is not sufficient to bring the measurements into agreement with the theoretical value of 2.1 ppm, indicating that the sensor not only experiences thermal effects due to the infrared absorption but also due to the associated electronics, mechanical and optical components of the sensor system.

4.2. Outdoor measurements

In order to study the effects of ambient temperature variations, we deployed the CH_4 sensor outside the Laser Science Group laboratory on the Rice University campus (Fig. 6) and used a 2.1 ppm standard cylinder to record variations of the CH_4 concentration level as the temperature varied during the day.

The experiments were carried out between May and June 2017 when the temperature in Houston varied from ~20 °C in the morning to >30 °C in the afternoon. The results of a typical test are shown in Fig. 7. Monitoring with CH_4 sensor was started at 7:00 AM and it was operated for ~9 h. When the sunlight was directly incident on the sensor at ~1:30 PM, the temperature increased significantly resulting in a decrease in the measurement of CH_4 concentration.

According to Fig. 7, the daily temperature variation significantly influences the CH_4 sensor measurement results. After compensation using Eq. (8), the variation of the measured concentration was reduced from 0.1033 ppm/°C to 0.0924 ppm/°C and was stable when the temperature varied from 24 to 40 °C.

Fig. 6. Photograph of the CH_4 sensor during environmental monitoring outside the Laser Science Group laboratory at Rice University campus in May and June 2017.

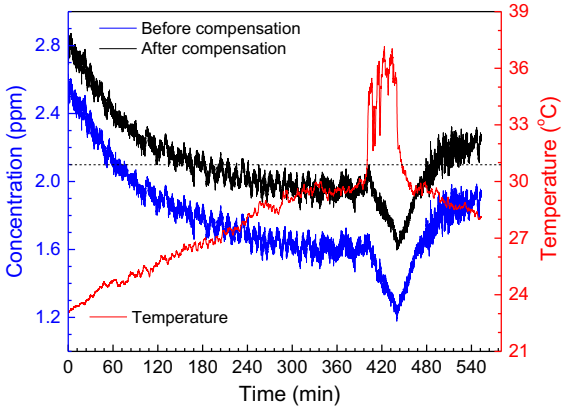

Fig. 7. CH_4 concentration measured before and after compensation, and temperature inside the MPGC by exposing the sensor to the sunlight for ~9 h.

5. Conclusions

In summary, analysis of thermal effects of a mid-infrared CH_4 sensor system using a TEC, CW ICL were investigated. The ICL targeted an interference-free CH_4 absorption line centered at 3334.38 nm and the pressure inside the MPGC was controlled at 100 Torr. The sensor performance in the laboratory at a constant temperature was measured for 5 h and its Allan deviation was ~2 ppbv with a 1 s averaging time. Influences of thermal effects on the sensor performance were numerically studied and a compensation technique was implemented. An environmental test chamber was employed to investigate the sensor response for a wide range of temperature. Furthermore, outdoor experiments were carried out at Rice University campus, where we monitored the sensor system performance under the influence of a wide atmospheric temperature variation. It was found that the sensor system not only experiences thermal effects due to the infrared absorption but also due to the associated electronics, mechanical and optical components.

Conflict of interest

This statement is to confirm that there is no conflict of interest of this manuscript with other parties.

Acknowledgements

The authors wish to express their gratitude to the DOE-ARPA-E awards, United States (DE-0000545, DE-0000547), a National Science Foundation, United States (NSF) (ERC MIRTHE award), a Welch Foundation grant, United States (C-0586), the National Natural Science Foundation of China (NSFC) (61307124, 61627823, 61775079), China Scholarship Council (20150844 0112), High School Outstanding Young Teacher Training Program of Guangdong Province, China (YQ2015071), Science and Technology Planning Project of Guangdong Province, China (2017A020216011), the Natural Science Foundation of Guangdong Province, China (2015A030313442), and Key Science and Technology "R&D" Program of Jilin Province, China (20180201046GX) for their generous support to this work.

References

[1] R.K. Pachauri, M.R. Allen, V.R. Barros, J. Broome, W. Cramer, R. Christ, N.K. Dubash, Climate change 2014: synthesis report, in: Contribution of Working Groups I, II and III to the fifth assessment report of the Intergovernmental Panel on Climate Change, IPCC, 2015, p. 151.
[2] D. Allen, Attributing atmospheric methane to anthropogenic emission sources, Acc. Chem. Res. 49 (2016) 1344–1350.
[3] G.K. Plattner, T. Stocker, P. Midgley, M. Tignor, IPCC expert meeting on the science of alternative metrics, IPCC Working Group I Technical Support Unit, Bern, 2009.
[4] EPA, Inventory of U.S. Greenhouse Gas Emissions and Sinks: 1990-2015, Washington, D.C., 2017.
[5] W. Ren, A. Farooq, D.F. Davidson, R.K. Hanson, CO concentration and temperature sensor for combustion gases using quantum-cascade laser absorption near 4.7 μm, Appl. Phys. B 107 (2012) 849–860.
[6] M.A. Bolshov, Y.A. Kuritsyn, V.V. Liger, V.R. Mironenko, Development of diode laser absorption spectroscopy method for determining temperature and concentration of molecules in remote object, Opt. Spectrosc. 110 (2011) 848–856.
[7] C.S. Goldenstein, C.L. Strand, I.A. Schultz, K. Sun, J.B. Jeffries, R.K. Hanson, Fitting of calibration-free scanned-wavelength-modulation spectroscopy spectra for determination of gas properties and absorption line shapes, 53 (2014) 356–367.
[8] I. Vurgaftman, W.W. Bewley, C.L. Canedy, C.S. Kim, M. Kim, C.D. Merritt, J. Abell, J.R. Lindle, J.R. Meyer, Rebalancing of internally generated carriers for mid-infrared interband cascade lasers with very low power consumption, Nat. Commun. 2 (2011) 585.
[9] K.M. Manfred, G.A.D. Ritchie, N. Lang, J. Ropcke, J.H. van Helden, Optical feedback cavity-enhanced absorption spectroscopy with a 3.24 um interband cascade laser, Appl. Phys. Lett. 106 (2015) 221106.
[10] J.H. Northern, S. O'Hagan, B. Fletcher, B. Gras, P. Ewart, C.S. Kim, M. Kim, C.D. Merritt, W.W. Bewley, C.L. Canedy, J. Abell, I. Vurgaftman, J.R. Meyer, Mid-infrared multi-mode absorption spectroscopy using interband cascade lasers for multi-species sensing, Opt. Lett. 40 (2015) 4186–4189.
[11] W. Ye, C. Li, C. Zheng, N.P. Sanchez, A.K. Gluszek, A.J. Hudzikowski, L. Dong, R.J. Griffin, F.K. Tittel, Mid-infrared dual-gas sensor for simultaneous detection of methane and ethane using a single continuous-wave inter band cascade laser, Opt. Exp. 24 (2016) 16973–16985.
[12] C. Li, L. Dong, C. Zheng, F.K. Tittel, Compact TDLAS based optical sensor for ppb-level ethane detection by use of a 3.34 μm room-temperature CW interband cascade laser, Sens. Actuat. B. Chem. 232 (2016) 188–194.
[13] L.S. Rothman, I.E. Gordon, Y. Babikov, A. Barbe, D.C. Benner, P.F. Bernath, A. Campargue, The HITRAN2012 molecular spectroscopic database, J. Quant. Spectrosc. Radiat. Transfer 130 (2013) 4–50.
[14] X. Zhou, X. Liu, J.B. Jeffries, R.K. Hanson, Development of a sensor for temperature and water concentration in combustion gases using a single tunable diode laser, Meas. Sci. Technol. 14 (2003) 1459.